Acquiring and Modeling of Si Solar-Cell Transient Response to Pulsed X-Ray

Lei Pan, Praneeth Kandlakunta, *Member, IEEE*, Matthew Van Zile, Xuezeng Dai, Jinsong Huang, John W. McClory, and Lei R. Cao, *Senior Member, IEEE*

***Abstract*— We report on the acquisition and modeling of the transient response of a commercial silicon (Si) solar cell using a benchtop pulsed X-ray source. The solar-cell transient output to the X-ray pulses was acquired under the dark and steady-state light illumination to mimic the practical operation of a solar cell under different light illumination levels. A solar-cell circuit model was created to develop a fundamental understanding of the transient current/voltage response of solar cell at read-out circuit level. The model was validated by a good agreement between the simulation and experimental results. It was found that the solar-cell resistance (R) and capacitance (C) depend on the light illumination, and the resulting variation in RC time constant significantly affects the solar-cell transient response. Thus, the solar cell produced different transient signals under different illumination intensities in response to the same X-ray pulse. The experimental data acquired in this work proves the feasibility of using solar panels for prompt detection of nuclear detonations, which also builds a practical mode of X-ray detection using a low-cost self-powered detector.**

***Index Terms*— Nuclear detonation detection, pulsed X-ray, solar cell, transient response.**

I. Introduction

THE prompt detection and identification of a nuclear detonation against a chemical denotation is critical for a fast response during the postdetonation nuclear forensics. Signatures of a nuclear detonation include shock waves, seismic waves, infrasound, thermal and ionizing radiation, electromagnetic pulse, and radioactive fallout [1], [2]. Networks of seismic, hydro-acoustic, and infrasound sensors may be serviceable for a fast off-site detection of nuclear detonation, but their effectiveness remains questionable, particularly in the case of surface and atmospheric detonations, where the sensor signal encounters a potentially high interference from that induced by an earthquake [3], [4]. Detection of radioactive particles and subsequent analysis using either air or ground sampling systems through on-site inspection is a relatively slow process. Existing urban infrastructure, such as the widely distributed and ubiquitous solar photovoltaic (PV) panels, may serve as potential sensors to detect a nuclear detonation, providing data that could be complementary or supplementary to that from any other sensor systems. The solar PV panels and solar array networks could provide valuable postdetonation forensics data at no additional capital, when compared to sensor systems built specifically for monitoring nuclear detonation. The feasibility of prompt detection of thermal radiation from a nuclear detonation using solar panels power distribution grid was studied recently [5]. While thermal radiation could also be released from chemical detonations, ionizing radiation is a unique signature of nuclear detonation, the detection of which provides a means for prompt identification. The large solar farms or even roof-top solar panels may potentially respond to the enormous amount of energy carried by ionizing radiations from a nuclear detonation, either by prompt interactions with X-rays, gamma-rays, neutrons, or by delayed effects such as neutron activation and radiation-induced damage.

It is known that a solar panel is built specifically to absorb solar radiation in the UV–visible–IR region of the electromagnetic spectrum. Unlike a semiconductor gamma-ray or neutron detector, a solar cell is not operated in reverse bias and therefore, has a very thin depletion region where electron–hole pairs generated by incident photons drift to the respective electrodes inducing current in an external circuit. While a thin depletion region is suitable to absorb visible photons that have short absorption lengths, photons of much shorter wavelength, that is, X-rays and gamma-rays have much deeper penetration lengths, thus generating e–h pairs across the entire solar-cell volume. To investigate the feasibility of a solar PV panel as a potential sensor of nuclear detonation, the response of a single PV element, that is, a solar cell to ionizing radiation such as X- and gamma-rays, and neutrons must be evaluated and understood first. For this purpose, a benchtop X-ray source may provide an ideal testbed to produce valuable data that facilitate the understanding of a solar-cell response at a read-out circuit level. Results from such analyses may provide a strong foundation to studies on a larger scale using larger experimental facilities and large-area PV panels. In the current

Manuscript received February 17, 2021; accepted March 15, 2021. Date of publication March 18, 2021; date of current version May 20, 2021. This work was supported by the Department of the Defense, Defense Threat Reduction Agency under Grant HDTRA1-19-1-0024.

Lei Pan, Praneeth Kandlakunta, and Lei R. Cao are with the Nuclear Engineering Program, Department of Mechanical and Aerospace Engineering, The Ohio State University, Columbus, OH 43210 USA (e-mail: pan.707@osu.edu; kandlakunta.1@osu.edu; cao.152@osu.edu).

Matthew Van Zile is with the OSU Nuclear Reactor Laboratory, The Ohio State University, Columbus, OH 43212 USA (e-mail: vanzile.3@osu.edu).

Xuezeng Dai and Jinsong Huang are with the Department of Applied Physical Sciences, The University of North Carolina at Chapel Hill, Chapel Hill, NC 27514 USA (e-mail: xuezeng@unc.edu; jhuang@unc.edu).

John W. McClory is with the Department of Engineering Physics, Air Force Institute of Technology, Wright-Patterson Air Force Base, OH 45433 USA (e-mail: jmcclory@afit.edu).

Color versions of one or more figures in this article are available at https://doi.org/10.1109/TNS.2021.3067193.

Digital Object Identifier 10.1109/TNS.2021.3067193

study, we focus on the silicon (Si) solar-cell steady-state and transient response to X-rays using a commercial off-the-shelf (COTS) laboratory-scale compact X-ray tube. Although originally motivated by the purpose of nuclear detonation detection, the work reported here could be supporting solar cells as potential X-ray sensors, complementary to the broad topic of semiconductor devices for X-ray detection. It must be noted, however, that the fundamental differences in design, fabrication, and operation between a solar cell and a typical semiconductor X-ray detector would lead to inherent variation in their response.

Semiconductor detectors (e.g., Si-, GaAs-, CdTe-, or CdZnTe-based) specifically designed for X-ray detection would have a higher sensitivity and a faster response (e.g., subnanosecond level) [6]–[9], because of the well-controlled fabrication process and operating environment (e.g., stable operating temperature and dark condition). Contrarily, the Si solar cells are most commonly made of polycrystalline Si and work under varying sunlight intensity. The light illumination level will have a significant impact on their response to X-rays. Experimental results of Si solar-cell response to pulsed laser illumination have been reported in [10]–[13]. However, the Si solar-cell response to pulsed X-rays has been rarely studied, with a lack of experimental data on its transient response, except for a few studies that only report Si solar-cell damage under pulsed X-ray irradiation [14]. In addition, a comprehensive study of the transient response of a Si solar cell to pulsed X-rays based on experimental analyses and circuit-level modeling and simulations has not yet been performed.

In this work, we experimentally evaluated the Si solar-cell response to pulsed X-rays both with and without light illumination, which demonstrated the capability and potential application of Si solar cells for the detection of transient X-ray radiation. A solar-cell equivalent-circuit simulation model was developed to analyze the experimental results and gain a fundamental understanding of the Si solar-cell transient current and voltage response at circuit level. The circuit model was validated by a good agreement between the simulation and measured transient response. Factors and conditions affecting Si solar-cell response to the same X-ray source input were analyzed. It is found that light illumination level and the associated *RC* effect significantly affect the output signal. Thus, the Si solar cell produced different responses to the pulsed X-ray source of same intensity at different light illumination levels.

II. Experimental Setup and Results

A. Experimental Setup

Our experimental setup consisted of an X-ray source (Amptek Mini-X transmission type X-ray tube with a silver target, tube voltage from 10 to 50 kV, tube current from 5 to 200 μA, and maximum power of 4 W), an X-ray chopper (Optical chopper system–Thorlabs MC2000, with chopper wheel replaced by a customized stainless-steel (304 SS) chopper wheel, chopping frequency 20–1000 Hz), a sunlight simulator (Ocean Optics HL-2000-HP, output power 8.8 mW), a light-tight metal box enclosure, an oscilloscope, and a

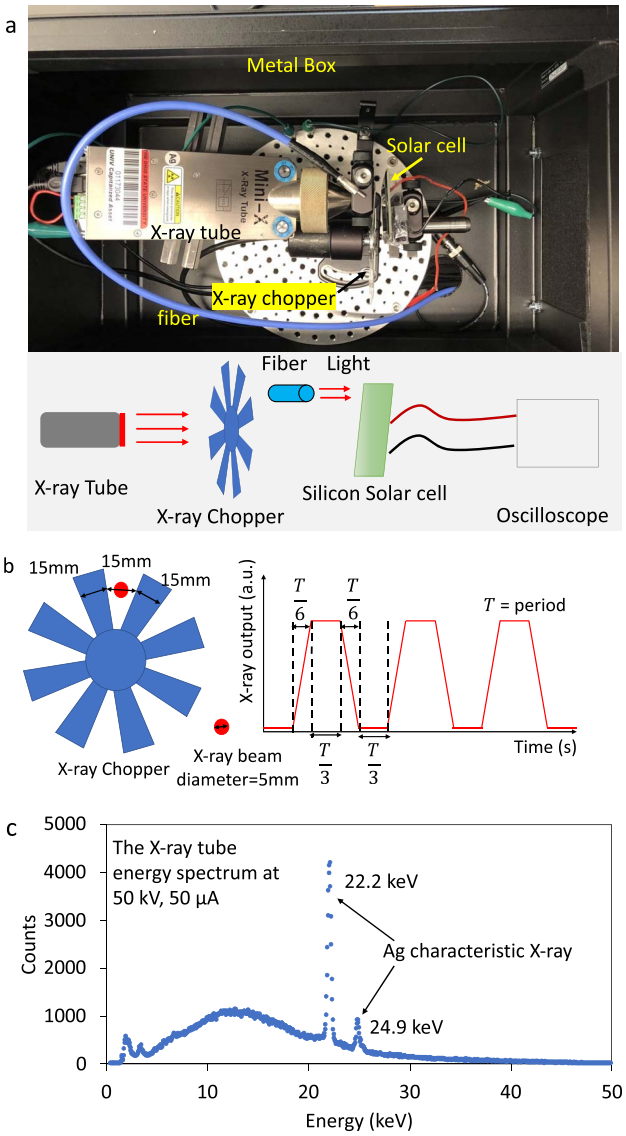

Fig. 1. Experimental setup for Si solar-cell transient response to pulsed X-ray testing. (a) Setup. (b) Parameters of chopper, X-ray beam, and pulsed X-ray signal. (c) X-ray tube energy spectrum at 50 kV, 50 μA.

commercial Si solar cell (Kitronik 3604) [Fig. 1(a)]. The X-ray tube, X-ray chopper, and the solar cell were all housed in the metal box to shield from ambient light and electromagnetic interference. An optical fiber was used to transmit the light from the sunlight simulator onto the solar cell in the light-tight box. The SS X-ray chopper wheel has a thickness of 0.762 mm, which attenuates ~99% of 30-keV and ~70% of 50-keV X-ray photons. The X-ray beam diameter is ~5 mm and the slot width between successive chopper blades at X-ray beam projection is ~15 mm, which gives rise to a trapezoid-like X-ray pulse [Fig. 1(b)]. Due to the nonuniformity of the beam profile, for example, beam shape, size, and beam intensity radial and angular distribution, the X-ray pulse shape deviates from that of an ideal trapezoid. However, for the purpose of this study, a trapezoid was considered to be a reasonable approximation to the true pulse shape to reduce the complexity of the simulation model. The duration of the trapezoidal flat top and bottom is each one-third of the pulse

period, and the time for pulse rise to the flat top and fall to the flat bottom, each is one-sixth of the period. The solar cell used in this study contains six subcells connected in series and is made of polycrystalline Si with dimensions of ~60 mm × 46 mm × 3 mm and an aperture area of 52 mm × 38 mm.

Although the direct response of a solar cell to the incident X-rays is photocurrent, in principle, either the current or voltage output can be used to study the transient response characteristics of the solar cell. Due to the fast transient nature of the incident X-rays and the resulting low photocurrent, an oscilloscope (Tektronix, MSO54, 2 GHz, 6.25 GS/s) with high sampling speed was used to capture the solar-cell transient response in the form of a measurable voltage signal, enabled by the 1 MΩ impedance channel of the oscilloscope. The energy spectrum of the X-ray source at a tube voltage of 50 kV and a tube current of 50 μA was calibrated with a Si p-i-n X-ray detector [Fig. 1(c)].

B. Experimental Results

To reproduce the operation of a solar PV panel under different sunlight conditions, such as a sunny/cloudy daytime, dark nighttime, and so on, the solar-cell transient response was studied under different light illumination intensities.

We first measured the output voltage response of a solar cell to pulsed X-rays under dark on 1-MΩ load resistance. In these measurements, the sunlight simulator was turned off and the metal enclosure was kept light-tight. Fig. 2(a) shows the measurement results obtained at different X-ray tube voltages from 20 to 50 kV (corresponding to different X-ray energies) for a constant tube current of 50 μA and a X-ray pulse frequency of 20 Hz. Results indicate a clear response of the solar cell to X-rays with the output voltage signal accurately reproducing the input X-ray pulse frequency of 20 Hz. The output voltage increases as the X-ray energy increases. However, the increment in output voltage relative to the increase in X-ray energy becomes smaller at higher X-ray energies, which is due to the lower sensitivity of Si to higher-energy X-ray photons and the relatively small spectral contribution of these high-energy X-ray photons (e.g., 40–50 keV) in the X-ray source energy spectrum [Fig. 1(c)].

Fig. 2(b) shows the measurement results obtained at different X-ray pulse frequencies for a fixed X-ray energy spectrum and intensity (40 kV, 50 μA). The X-ray beam irradiated the solar cell at an arbitrarily selected area. The solar cell produced an output voltage with the same frequency as the input X-ray pulse and the peak-to-peak value of the output voltage decreased with increasing frequency, whereas the centerline of the waveform remained unchanged. The minimum and maximum solar-cell output voltages in response to steady-state X-ray flux (40 kV, 50 μA) were also measured. In these measurements, the X-ray beam was turned on, and the chopper wheel was not rotated, so that the minimum and maximum steady-state responses of the solar cell was measured when the X-ray beam was completely covered and uncovered by a chopper blade, respectively, by adjusting the chopper blade position. It is noticed that the steady-state

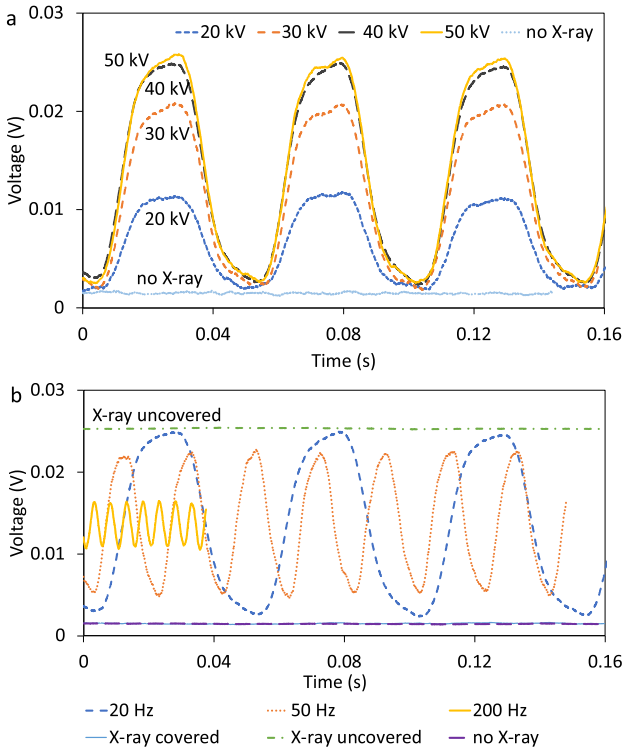

Fig. 2. Experimental results of Si solar-cell transient response to pulsed X-ray with sunlight simulator off. (a) Si solar-cell output voltage on 1-MΩ load resistance at different X-ray tube voltage with fixed X-ray tube current of 50 μA and fixed pulsed X-ray frequency of 20 Hz. (b) Si solar-cell output voltage on 1-MΩ load resistance at different pulsed X-ray frequencies with fixed X-ray tube voltage, current of 40 kV, 50 μA. "No X-ray" stands for measurement taken with X-ray tube off. "X-ray covered/uncovered" stands for measurement taken with X-ray tube on and the X-ray beam covered/uncovered by a chopper blade. The lines of "no X-ray" and "X-ray covered" are almost identical.

maximum or minimum output voltage is larger or smaller than the peak values of the output voltage for X-ray pulse frequency from 20 to 200 Hz. This is a consequence of the relatively large *RC* constants under dark conditions, which is discussed in Section III-C. Interesting to note is the solar-cell minimum output voltage obtained with X-rays blocked by the chopper blade, which is almost identical to the voltage measured with X-ray beam turned off. This indicates that the SS chopper blade fully blocked the X-rays and X-ray scattering has a negligible effect on the solar-cell output. This is to be expected because the X-ray energy is too low to favor Compton scattering events. To reproduce the above results, measurements were performed for 40-kV, 50-μA X-rays, changing the X-ray beam irradiation location by adjusting the solar-cell position relative to the X-ray beam exit. The measurement yielded essentially the same response as shown in Fig. 2(b), however, with a different signal amplitude (i.e., a steady-state maximum voltage of 35 mV). This is attributed to the solar-cell geometric variation, for example, caused by the presence of electrode fingers on the top surface.

The solar-cell output voltage response to pulsed X-rays was also measured under light illumination using the same setup as under the dark, with the only difference of powering on the sunlight simulator. Fig. 3 shows the results obtained for 40-kV, 50-μA pulsed X-rays at different frequencies from

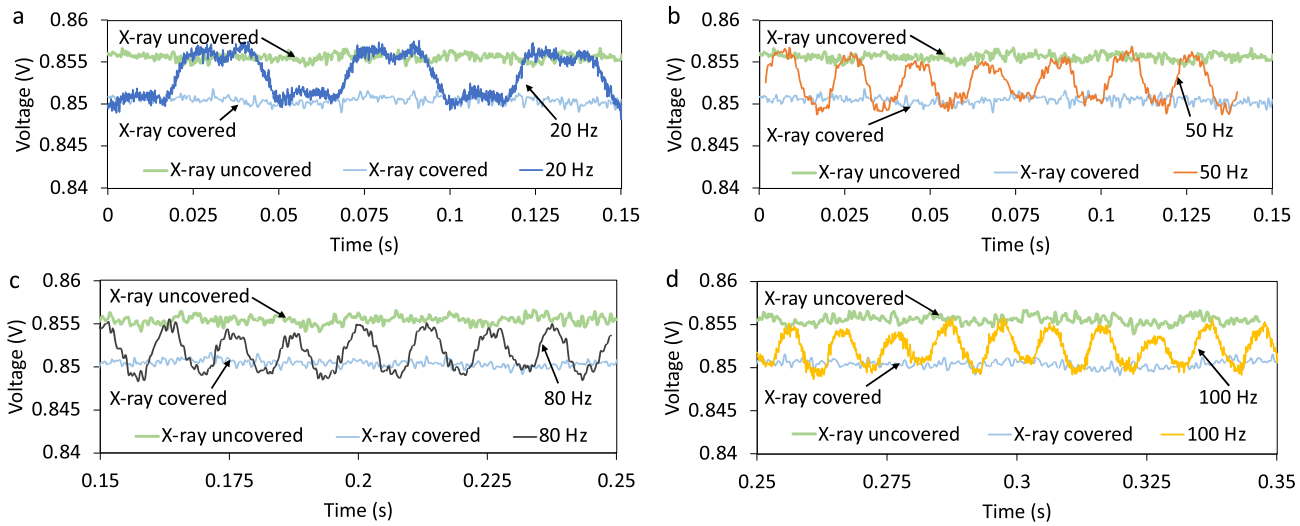

Fig. 3. Experimental results of Si solar-cell output voltage to pulsed X-ray with sunlight simulator on and at different pulsed X-ray frequency of (a) 20 Hz, (b) 50 Hz, (c) 80 Hz, and (d) 100 Hz. The load resistance is 1 MΩ. X-ray tube voltage and current are fixed at 40 kV and 50 μA, respectively.

20 to 100 Hz. The centerline of the output voltage shifts to a higher value than that under dark, which is due to the steady-state light illumination. It is noticed that the shape of the output voltage under light illumination is closer to trapezoidal than that under dark. Furthermore, the peak-to-peak value of the output voltage under light illumination does not decrease with increasing frequency. The peak values are equal to the steady-state maximum/minimum output voltage, which is attributed to the relatively small RC constant under light illumination as discussed in Section III-C.

III. Solar-Cell Modeling

A. Solar-Cell Model for Transient Signal Simulation

To gain a fundamental understanding of solar-cell transient response, we developed a solar-cell equivalent-circuit model and simulated its dynamic behavior. While the model was used to evaluate the solar-cell current/voltage response to pulsed X-rays and better understand the experimental results, it could also provide insights into solar-cell response to transient inputs of different temporal characteristics, such as a triangular, square, or a pulsewidth-modulated waveform.

Different models have been reported for calculation or simulation of solar-cell parameters, for example, single-diode model, double-diode model, and so on [15]–[18]. However, none of these models focus on the solar-cell transient behavior and therefore, do not take the solar-cell capacitance into account. In this study, a typical single-diode solar-cell model was adopted that included cell capacitance C along with a photocurrent source $I_{\rm ph}$, a diode shunt resistance $R_{\rm sh}$, and series resistance $R_{\rm s}$ [Fig. 4(a)]. Our model considered the physical process starting right from the moment the X-ray photons impinge on the solar cell. The time for charge-generation process due to energy deposition of X-ray photons can be neglected as the time for X-ray photon interaction (predominantly photoelectric absorption) causing the release of a fast electron, and subsequent electron–hole pair generation, is extremely short. As a consequence, the rate of X-ray illumination and the rate of charge generation can be modeled as two processes with no time lag. In other words, the rate of charge generation would have the exact same temporal characteristics as that of the incident X-rays. The steady-state photogenerated current in a p-n diode can be expressed as $J_L = eG_LW + eG_LL_{\rm n} + eG_LL_{\rm p}$, where J_L is the photocurrent per unit area, e is the elementary charge, G_L is the rate of charge generation per unit volume, W is the depletion region width, and $L_{\rm n}$ and $L_{\rm p}$ are the diffusion lengths of minority electrons in the p region and minority holes in the n region, respectively [19]. From the above equation, since W, $L_{\rm n}$, and $L_{\rm p}$ are time-independent, the temporal characteristics of J_L are the same as that of G_L, and therefore, also identical to that of the incident X-rays without any time lag. Therefore, the photocurrent source $I_{\rm ph}$ ($I_{\rm ph} = J_L * A$, A is the diode area) in the model has the same magnitude as the steady-state photocurrent and the same temporal behavior as that of the incident X-rays. On the contrary, the output current/voltage has a different temporal behavior from that of the input photocurrent source. From a circuitry point of view, the solar-cell output current/voltage has a slower response to the photocurrent source as a consequence of the RC effect resulting from the solar-cell capacitance and resistance. From a fundamental physics perspective, the photocurrent J_L induced in a solar cell is dominated by the diffusion current component $eG_LL_{\rm n} + eG_LL_{\rm p}$ against drift current component eG_LW, owing to the extremely thin depletion region in a solar cell ($\leq$1 μm). The diffusion current is determined by the minority charge carrier concentration in the quasi-neutral regions within a "diffusion length" distance from the depletion region. It takes time for the minority carrier concentration to change as a result of charge generation by X-ray photon illumination. In other words, the solar-cell diffusion capacitance, which is the rate of change of excess minority carrier concentration with respect to the cell forward-bias voltage, has a significant effect on its response time. For an ideal p-n junction solar cell, the rise time of solar-cell short-circuit current in response to a step input X-ray illumination is at the same level of the minority charge carrier lifetime. The relation between the photocurrent

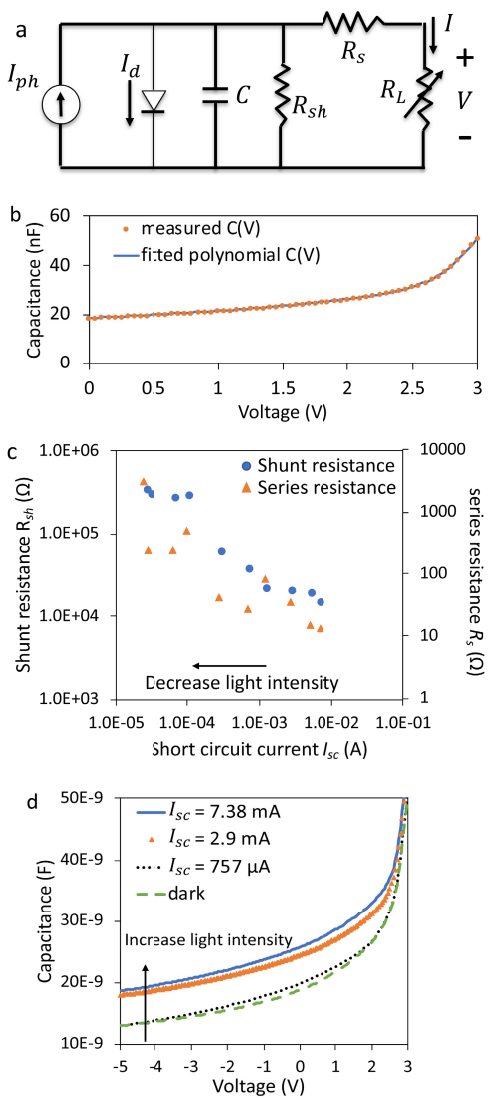

Fig. 4. Solar-cell circuit model for transient signal simulation. (a) Single-diode solar-cell circuit model. (b) Measured and fitted capacitance–voltage (C–V) curve of the solar cell. (c) Shunt and series resistance extracted using the method of Phang *et al.* [18]. (d) Capacitance–voltage curves measured at different light illumination intensities represented by different short-circuit currents.

$I_{\rm ph}$ and the output current I that was also the current measured experimentally can be expressed as the following equation:

$$I_{\rm ph} - I_0\left(\exp\left(\frac{eI(R_{\rm s}+R_{\rm L})}{nkT}\right)-1\right) - \frac{I(R_{\rm s}+R_{\rm L})}{R_{\rm sh}} = (R_{\rm s}+R_{\rm L})C\frac{dI}{dt}+I \quad (1)$$

where $I_0(\exp(eI(R_{\rm s}+R_{\rm L})/nkT)-1)$ is the diode forward-biased current $I_{\rm d}$, I_0 is the reverse saturation current, n is the diode ideality factor, k is Boltzmann's constant, T is the absolute temperature, and $R_{\rm L}$ is the solar-cell load resistance. The output voltage V can be obtained as $I \times R_{\rm L}$. To solve (1) for the output current I or output voltage V as a function of time, the cell parameters I_0, n, $R_{\rm s}$, $R_{\rm sh}$, and C, as well as $I_{\rm ph}$ must be estimated first under certain illumination condition and a given $R_{\rm L}$ value. These parameters could be estimated from an I–V curve using the method proposed by Phang *et al.* [18], while other methods may also be applicable [17]. Since the cell capacitance depends on the applied bias voltage [20], [21], it was modeled as a function of bias voltage using a polynomial fit to the experimental C–V curve [Fig. 4(b)]. It has been reported that the Si solar-cell parameters (i.e., I_0, n, $R_{\rm s}$, $R_{\rm sh}$) depend on the illumination intensity [22], [23]. Therefore, the shunt/series resistance and capacitance of the solar cell were determined at different light illuminations represented by different short-circuit currents in Fig. 4(c) and (d). As the light intensity decreases, both the shunt and series resistances increase, whereas the capacitance decreases. The cell parameters in the model may be approximated as constants under small changes in the illumination. However, for a significant variation in the illumination level, the cell parameters must be represented as illumination-dependent to ensure model accuracy. In this study, the solar-cell equivalent circuit was modeled using Simulink (The MathWorks, Inc.) (Fig. 5) to calculate both voltage and current outputs under variable load resistance.

B. Model Validation

The solar-cell voltage response to pulsed X-rays under light illumination confirmed the intuition that the contribution of X-rays to the output voltage was much smaller compared to that of the incident light. Fig. 3 shows the small increment in voltage (peak-to-peak ~5 mV) induced by X-rays relative to the much higher baseline (~850 mV) due to steady light illumination. It can, therefore, be assumed that the cell parameters remained constant during pulsed X-ray illumination. The I–V curves were also measured under steady-state light illumination when the X-ray beam was both completely uncovered and covered by a chopper blade at a X-ray tube voltage of 40 kV and a current of 50 μA (Fig. 6). The short-circuit current $I_{\rm SC}$ and open-circuit voltage $V_{\rm OC}$ measured with X-ray illumination are slightly larger than when the X-ray beam was covered, which indicates the effect of X-ray illumination. However, there was no significant difference between cell parameters extracted using the two I–V curves (see Fig. 6 caption), which validated our assumption that the cell parameters were constant during pulsed X-ray illumination. However, the estimated parameter values do not fall into the typical range of the Si solar-cell parameters (e.g., an ideality factor of 1–2). A possible explanation is that the light illumination in these measurements was much smaller than one sun illumination and was localized to only a small area on the solar cell due to the small area of the optical fiber exit ~$\pi \times 1.5^2$ mm^2). The simulated I–V curves using the extracted parameters agree well with the experimentally measured I–V curves with only a slight discrepancy. The solar-cell parameters thus obtained using the I–V measurements, under light illumination with both X-rays uncovered and covered, were fed into the Simulink model. Simulations run with a load resistance $R_{\rm L} = 1$ MΩ produced a steady-state output voltage of 862 and 857 mV, which agreed well with the experimentally measured values of 856 and 850 mV, under light illumination with X-ray beam uncovered and covered, respectively. For the simulations of solar-cell response to

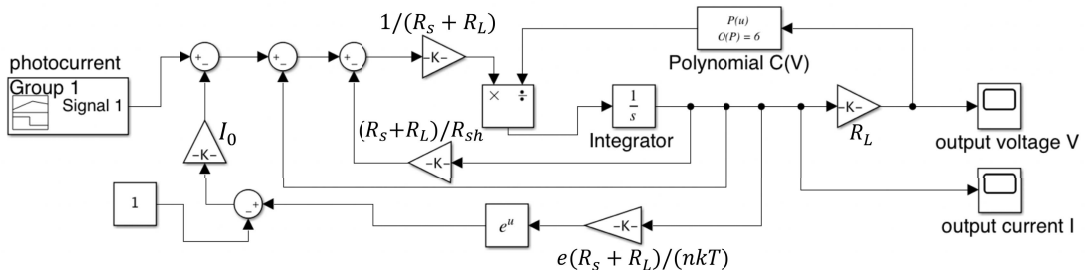

Fig. 5. Simulink model for solar-cell transient signal simulation.

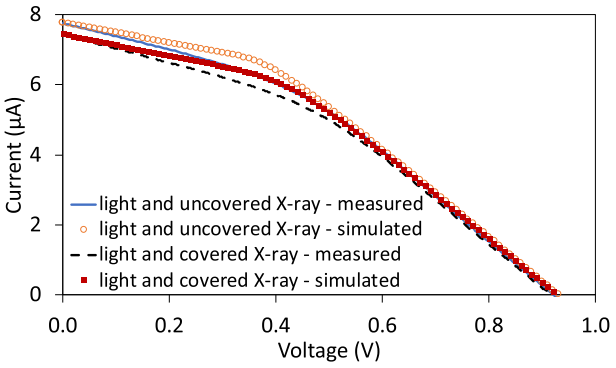

Fig. 6. Measured and simulated Si solar-cell I–V curves under light illumination. The X-ray tube voltage and current are 40 kV and 50 μA, respectively. "Uncovered X-ray" and "covered X-ray" stand for X-ray beam completely uncovered and covered by a chopper blade, respectively. The cell parameters extracted from the I–V curve of "light and uncovered X-ray-measured" are $n = 0.523$, $I_0 = 3.24\text{E-}28$ A, $R_{\text{sh}} = 2.8\text{E}5\ \Omega$, $R_{\text{s}} = 7.66\text{E}4\ \Omega$, and $I_{\text{ph}} = 9.84\ \mu$A. The cell parameters extracted from the I–V curve of "light and covered X-ray-measured" are $n = 0.714$, $I_0 = 3.86\text{E-}28$ A, $R_{\text{sh}} = 2.5\text{E}5\ \Omega$, $R_{\text{s}} = 7.57\text{E}4\ \Omega$, and $I_{\text{ph}} = 9.67\ \mu$A.

pulsed X-rays at frequency from 20 to 200 Hz, the cell parameters obtained from the I–V measurement under light illumination with X-rays uncovered were used in the model. The steady-state photocurrent input to the model for both X-ray beam uncovered and covered conditions was calculated in turn using the corresponding measured steady-state output voltage shown in Fig. 3. The steady-state photocurrent values thus calculated were used as the high and low values of the trapezoidal photocurrent input in the model simulating a pulsed X-ray source. Using the trapezoidal waveform to model the input photocurrent, the solar-cell output voltage on 1-MΩ load resistance was calculated for different X-ray pulse frequencies. The simulation results indicated trapezoidal shape of the output voltage pulses, which agreed very closely with the measured output voltage [Fig. 7(a)–(d)]. Results indicate the accuracy of the model in simulating a solar-cell transient response to pulsed X-rays under a steady light illumination. The results, further, validate the model for its applicability to simulate other scenarios with good precision.

To confirm the validity of the model and extend its application to simulate other environments, simulations were performed to evaluate the solar-cell response to pulsed X-rays under dark. However, in this case, the cell parameters estimated from the I–V curve under light illumination cannot be used due to their dependence on illumination intensity. Therefore, the I–V measurements were repeated with both X-ray beam covered and uncovered under dark. The results once again indicate the effect of X-ray illumination on solar cell (X-ray tube voltage at 40 kV and current at 50 μA) [Fig. 8(a)]. However, the cell parameters obtained from I–V measurements using Phang *et al.*'s [18] method were unrealistic, for example, a negative R_{s} value, which was found to be due to the extremely low illumination intensity of X-rays alone compared to that of light, falling outside the range of applicability of the method. Given the difficulty in finding a suitable set of cell parameters at such low illumination level, we gradually increased the illumination level from dark until a level at which the corresponding I–V curve produced acceptable cell parameters. Using the cell parameters obtained at such relatively higher illumination level, the model was expected to produce simulation results in a reasonable agreement with the measured results under dark.

Following this method, a set of cell parameters were extracted from the I–V curve measured at a relatively higher light illumination level [Fig. 8(b)]. The I–V curve fitted using these parameters agreed well with the experimental I–V curve. The cell parameters were then fed to the Simulink model for the simulation of solar-cell response to pulsed X-rays under dark. As earlier, the high and low values of the trapezoidal photocurrent source in the model were derived from the model using the experimentally measured steady-state output voltage under dark with the X-ray uncovered and covered, respectively, as shown in Fig. 2(b). Using the trapezoidal photocurrent input in the model, simulations were performed to evaluate the solar-cell output voltage at different X-ray pulse frequencies. The simulation results show a decreasing peak-to-peak value of the output voltage as frequency increases, which agrees with the experimental results [Fig. 8(c)–(f)]. There is, however, a notable difference between the simulated and measured peak-to-peak values. This is expected because the cell parameters were derived at a relatively higher illumination level caused by light rather than at the actual X-ray illumination alone.

Despite the difficulty in determining cell parameters from the I–V measurement at such a low X-ray illumination level, a set of cell parameters could still be found, in principle that could produce simulation results with lesser quantitative difference from measured results, and further support the model validity for pulsed X-ray simulations under dark. Comparison of the pulsed X-ray measurement results under dark with those under light illumination reveals that the decreasing peak-to-peak output voltage under dark [Fig. 2(b)] against the constant peak-to-peak output voltage under light, with

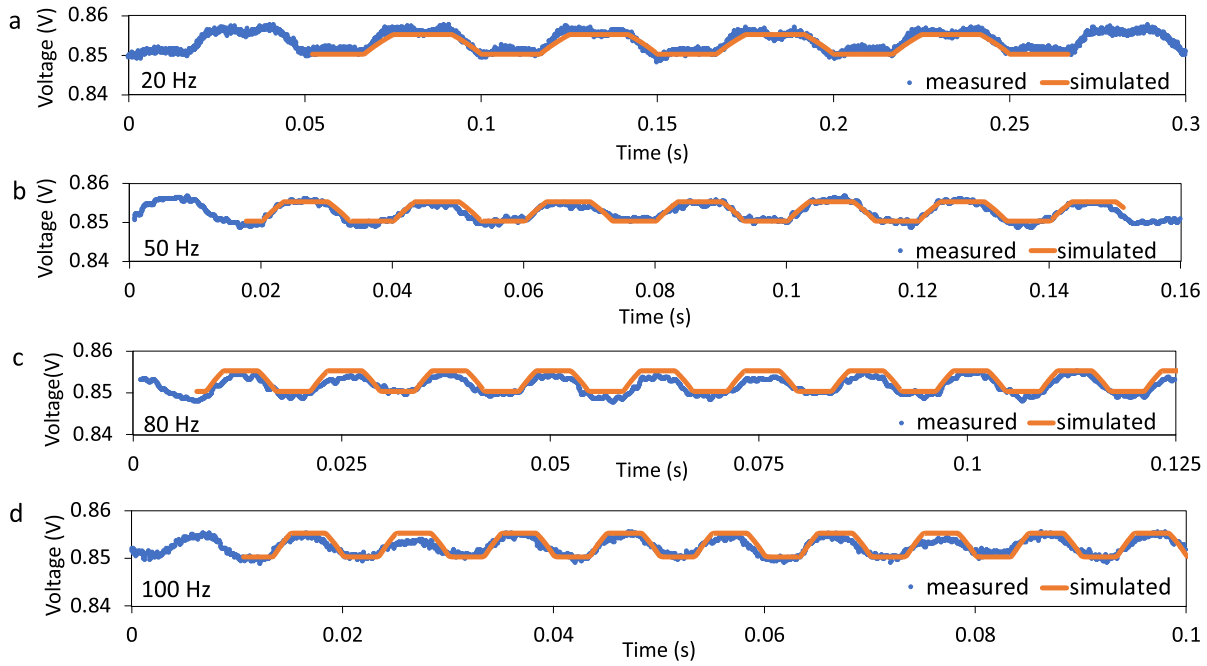

Fig. 7. Measured and simulated Si solar-cell output voltage on 1-MΩ load resistance in response to pulsed X-rays under light illumination. Results are shown at different pulsed X-ray frequencies of (a) 20 Hz, (b) 50 Hz, (c) 80 Hz, and (d) 100 Hz. X-ray tube voltage and current were kept constant at 40 kV and 50 μA, respectively.

increasing frequency (Fig. 3), is a result of a larger solar-cell RC constant under dark. The larger RC constant is manifested in the slower output voltage response under dark, where the output voltage has a settling time larger than the input pulse durations. A larger RC constant at lower light illumination is also demonstrated by the measured shunt/series resistance and capacitance results shown in Fig. 4(c) and (d). Based on these observations, we manually adjusted the cell parameter values originally extracted at a relatively high illumination level to account for larger RC while achieving a better approximation to the parameters at low X-ray illumination level under dark. Accordingly, the R_{sh} in the model was increased to 350 kΩ, whereas all other cell parameters shown in Fig. 8(b) were unchanged. To apply the model with increased R_{sh}, the high and low values of the trapezoidal photocurrent source were recalculated at this R_{sh} using the model following the same procedure as before. The modified model resulted in a smaller quantitative difference between the simulation and the experimental results (Fig. 9), which proves the validity of the model for simulating solar cell response to pulsed X-rays under dark.

C. Discussion and Estimation of Solar Panel Output

Both the experimental and simulation results indicate that the Si solar-cell response to the same pulsed X-ray input varies with the light illumination level due to variation in the corresponding RC constant. Such variation in the solar-cell transient response is significant at higher pulse frequencies. The output voltage under light illumination has nearly the same trapezoidal shape as that of the input X-ray pulses. Furthermore, the steady-state maximum and minimum output voltages corresponding to X-ray beam uncovered and covered conditions, respectively, are equal to the peak values of the output voltage at all frequencies (Fig. 3), which is due to the relatively small RC constant under light illumination. In contrast, the output voltage under dark has a shape that deviates from trapezoidal and a peak-to-peak value that decreases with increasing frequency [Fig. 2(b)], which is a consequence of relatively large RC constant without light illumination. In addition, the output voltage increment for the same steady-state X-ray input, under light illumination, that is, ∼5 mV (Fig. 3), is smaller than under dark, that is, ∼25 mV [Fig. 2(b)]. This is explained by the relationship between open-circuit voltage and input photocurrent $V_{\text{oc}} = (nkT/e)Ln(1 + I_{\text{ph}}/I_0)$ [19]. The open-circuit voltage (V_{oc}) increases logarithmically with the photocurrent (I_{ph}), so the same photocurrent increment (ΔI_{ph}), corresponding to the same X-ray input, would produce a smaller open-circuit voltage increment (ΔV_{oc}) at higher illumination level (higher I_{ph}). The output voltage on 1-MΩ load resistance is essentially close to the open-circuit voltage.

The model may be used to predict solar-cell response to X-ray burst from a nuclear denotation, given that the duration and intensity of the X-ray pulse is known, which can be derived from a suitable analysis and/or simulation of the burst. In this work, we studied the X-ray detection capability of a single Si solar-cell device using a simple laboratory setup of a compact X-ray source. However, since a solar-cell device is the fundamental constituent of large-area solar panels or solar arrays, the experimental data obtained from this work may be extended to evaluate their feasibility for the detection of X-rays from a nuclear denotation. Such a scale-up results would only be meaningful if an estimate of the air dose rate and energy distribution of X-rays from nuclear denotation, as well as the

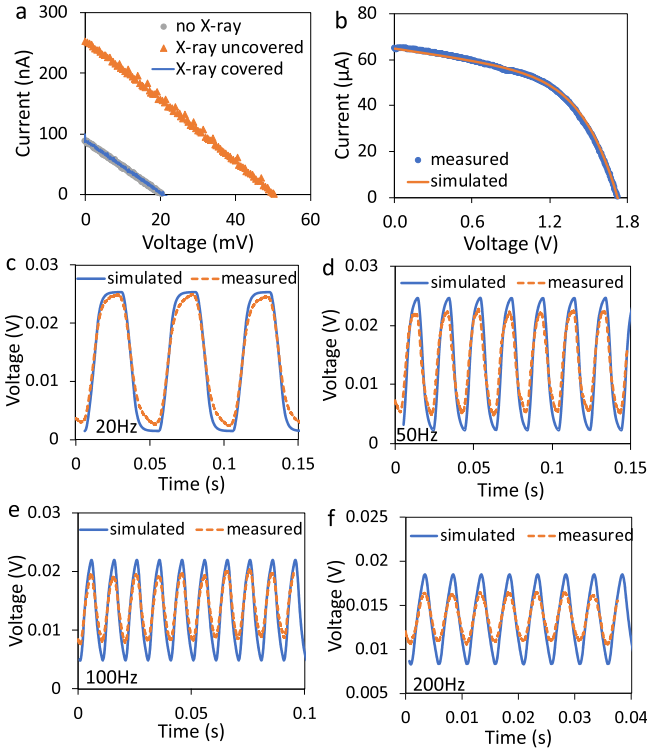

Fig. 8. Comparison of measured and simulated Si solar-cell I–V curves and output voltage to pulsed X-ray with sunlight simulator off. (a) I–V curves measured with X-ray beam completely uncovered/covered by a chopper blade (X-ray tube voltage 40 kV, current 50 μA). (b) Measured and simulated I–V curves at an arbitrarily selected light illumination level. The cell parameters extracted are n = 10.4, I_0 = 7.66E-8 A, R_{sh} = 1.43E5 Ω, R_s = 387 Ω, and I_{ph} = 64.9 μA. Measured and simulated Si solar-cell output voltage on 1-MΩ load resistance at fixed X-ray tube voltage, current of 40 kV, 50 μA, using the cell parameters extracted in (b), at different pulsed X-ray frequency of (c) 20 Hz, (d) 50 Hz, (e) 100 Hz, and (f) 200 Hz.

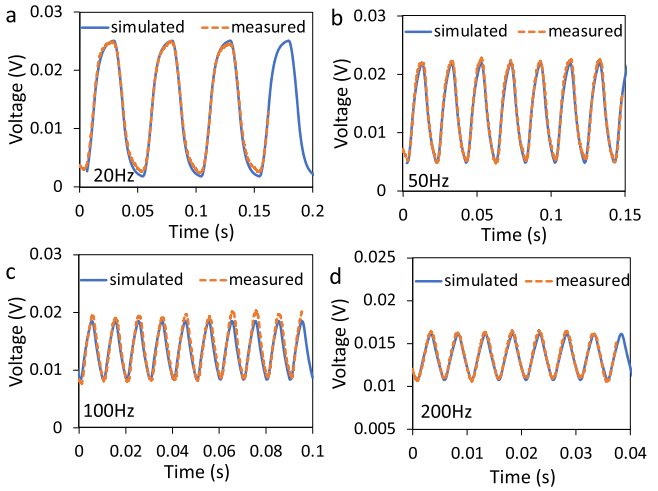

Fig. 9. Modified parameters applied to compare the measured and simulated Si solar-cell output voltage to pulsed X-ray with sunlight simulator off. Measured and simulated Si solar-cell output voltage on 1-MΩ load resistance at fixed X-ray tube voltage and current of 40 kV and 50 μA, respectively, using modified cell parameters, at different pulsed X-ray frequency of (a) 20 Hz, (b) 50 Hz, (c) 100 Hz, and (d) 200 Hz.

scale and design factors used in practical commercial solar arrays are available.

The air dose rate of X-rays (40 kV, 50 μA) used in our study was measured by a Fluke Biomedical RaySafe 452 dosimeter to be ∼20 μGy/s at the location of the solar cell. The corresponding X-ray photocurrent was measured to be 160 nA for an effective solar-cell area (circular of diameter ∼5 mm) irradiated by the X-rays, which results in a photocurrent density of ∼815 nA/cm^2. According to [1], a typical fission-based nuclear denotation of the air-burst kind with 20 kilotons explosion yield (explosion yield of the "Fat Man" is ∼21 kilotons) produces a tissue dose of ∼300 rad by ionizing photons in ∼10 s at ∼1.5 km away from the detonation point. This corresponds to an air dose rate of ∼276 mGy/s, produced by ionizing radiations with an energy and temporal distribution that could be derived from simulations. For an X-ray energy distribution similar to that in Fig. 1(c), an X-ray air dose rate of ∼276 mGy/s would yield a photocurrent density of ∼12 mA/cm^2 based on the current study. In comparison, a typical commercial solar cell produces a current of ∼30 mA/cm^2 at peak 1 sun illumination. The power output change of a solar farm due to a change in the net photocurrent density would cause a corresponding measurable change of power in the grid that can be monitored remotely, as demonstrated in [5]. More accurate data, for example, on the sequence of radiation events at solar panel/farm location, and their energy and temporal distribution may be extracted using an accurate profile of nuclear denotation in a simulation model considering the detonation yield, device design, topography, and so on.

IV. Conclusion

In this work, we investigated the transient response of a Si solar cell to X-rays using a laboratory-scale pulsed X-ray source. The Si solar cell produced a clear response to pulsed X-rays of varying X-ray energy and pulse frequency, both under dark and light illumination. A solar-cell circuit model was developed to study the transient response at different light illumination levels. The model was validated by a good agreement between the simulation and the experimental results. The light illumination and thus, the corresponding RC constant affected the solar-cell transient response, resulting in different transient characteristics for the same pulsed X-ray input at different illumination levels.

The current study enabled a fundamental understanding of the solar-cell transient output at the circuit level, while also supplementing the evaluation of Si solar cell as a potential X-ray detector. The capability of a Si solar cell to detect transient X-ray radiation for prompt identification of a nuclear detonation was also demonstrated by the preliminary results in this study. Evaluation of large-area solar panels for the detection of ionizing radiation from a nuclear detonation will be part of our future work and will involve irradiation of the solar panels by a much stronger pulsed X-ray source, such as the facility at Sandia National Laboratory [24], [25]. In addition, the energy and temporal distributions of ionizing radiations from a nuclear detonation will be calculated using simulations of different scenarios to further the evaluation of Si solar panels for the prompt detection of nuclear detonation.

ACKNOWLEDGMENT

The authors would like to thank Dr. Padhraic Mulligan for acquiring X-ray energy spectrum when he was a PhD student at OSU. They would also like to thank Dr. Richard Harrison and Dr. Jeremy Osborn at the Sandia National Laboratory for the constructive discussions. The content or the information presented does not necessarily reflect the position or the policy of the federal government, and no official endorsement should be inferred.

REFERENCES

[1] S. Glasstone and P. J. Dolan, The effects of nuclear weapons, vol. 50, no. 3. Richmond, VA, USA: US Department of Defense, 1977.

[2] R. Stone, "Surprise nuclear strike? Here's how we'll figure out who did it," *Science*, Mar. 2016. [Online]. Available: https://www.sciencemag.org/news/2016/03/surprise-nuclear-strike-heres-how-well-figure-out-who-did-it

[3] C. R. Carrigan *et al.*, "Delayed signatures of underground nuclear explosions," *Sci. Rep.*, vol. 6, no. 1, pp. 1–9, Sep. 2016, doi: 10.1038/srep23032.

[4] T. Bache, "Estimating the yield of underground nuclear explosions," *Bull. Seismolog. Soc. Amer.*, vol. 72, no. 6B, pp. S131–S168, 1982.

[5] Z. K. Pecenak, J. Kleissl, and E. Lam, "Detection of a surface detonated nuclear weapon using a photovoltaic rich distribution grid," in *Proc. IEEE Power Energy Soc. Gen. Meeting (PESGM)*, Aug. 2018, pp. 1–5, doi: 10.1109/PESGM.2018.8586123.

[6] Q. Looker, M. G. Wood, P. W. Lake, J. K. Kim, and D. K. Serkland, "GaAs X-ray detectors with sub-nanosecond temporal response," *Rev. Sci. Instrum.*, vol. 90, no. 11, Nov. 2019, Art. no. 113505.

[7] S. Tokuda, H. Kishihara, S. Adachi, and T. Sato, "Improvement of the temporal response and output uniformity of polycrystalline CdZnTe films for high-sensitivity X-ray imaging," *Proc. SPIE*, vol. 5030, pp. 861–870, Jun. 2003.

[8] Q. Looker, B. A. Aguirre, M. E. Hoenk, A. D. Jewell, M. O. Sanchez, and B. D. Tierney, "Superlattice-enhanced silicon soft X-ray and charged particle detectors with nanosecond time response," *Nucl. Instrum. Meth. Phys. Res. A, Accel. Spectrom. Detect. Assoc. Equip.*, vol. 916, pp. 148–153, Feb. 2019.

[9] Q. Looker, M. G. Wood, A. Miceli, M. Niraula, K. Yasuda, and J. L. Porter, "Synchrotron characterization of high-Z, current-mode X-ray detectors," *Rev. Sci. Instrum.*, vol. 91, no. 2, 2020, Art. no. 23509.

[10] J. A. Yater, R. A. Lowe, P. P. Jenkins, and G. A. Landis, "Pulsed laser illumination of photovoltaic cells," in *Proc. IEEE 1st World Conf. Photovoltaic Energy Convers. WCPEC (a Joint Conf. PVSC, PVSEC PSEC)*, Dec. 1994, pp. 2177–2180.

[11] T. Dennis, "Saturation in solar cells from ultra-fast pulsed-laser illumination," in *Proc. IEEE 44th Photovoltaic Spec. Conf., PVSC*, Jun. 2017, pp. 3023–3026, doi: 10.1109/PVSC.2017.8366716.

[12] R. A. Lowe, G. A. Landis, and P. Jenkins, "Response of photovoltaic cells to pulsed laser illumination," *IEEE Trans. Electron Devices*, vol. 42, no. 4, pp. 744–751, Apr. 1995, doi: 10.1109/16.372080.

[13] R. K. Jain and G. A. Landis, "Transient response of gallium arsenide and silicon solar cells under lazer pulse," *Solid. State. Electron.*, vol. 42, no. 11, pp. 1981–1983, 1998, doi: 10.1016/S0038-1101(98)00143-9.

[14] P. P. Jenkins *et al.*, "Nuclear weapons effects testing of solar cells using the national ignition facility (NIF)," in *Proc. 35th IEEE Photovoltaic Specialists Conf.*, Jun. 2010, Art. no. 002550, doi: 10.1109/PVSC.2010.5614573.

[15] P. Saha, S. Kumar, S. K. Nayak, and H. S. Sahu, "Parameter estimation of double diode photo-voltaic module," in *Proc. 1st Conf. Power, Dielectric Energy Manage. NERIST (ICPDEN)*, Jan. 2015, pp. 1–4, doi: 10.1109/ICPDEN.2015.7084502.

[16] D. S. H. Chan and J. C. H. Phang, "Analytical methods for the extraction of solar-cell single- and double-diode model parameters from I-V characteristics," *IEEE Trans. Electron Devices*, vol. 34, no. 2, pp. 286–293, Feb. 1987, doi: 10.1109/T-ED.1987.22920.

[17] A. M. Humada, M. Hojabri, S. Mekhilef, and H. M. Hamada, "Solar cell parameters extraction based on single and double-diode models: A review," *Renew. Sustain. Energy Rev.*, vol. 56, pp. 494–509, Apr. 2016, doi: 10.1016/j.rser.2015.11.051.

[18] J. C. H. Phang, D. S. H. Chan, and J. R. Phillips, "Accurate analytical method for the extraction of solar cell model parameters," *Electron. Lett.*, vol. 20, no. 10, p. 406, 1984, doi: 10.1049/el:19840281.

[19] D. A. Neamen, *Semiconductor Physics and Devices: Basic Principles*. New York, NY, USA: McGraw-Hill, 2012.

[20] G. Friesen and H. A. Ossenbrink, "Capacitance effects in high-efficiency cells," *Sol. Energy Mater. Sol. Cells*, vol. 48, nos. 1–4, pp. 77–83, 1997, doi: 10.1016/S0927-0248(97)00072-X.

[21] S. K. Sharma, D. Pavithra, G. Sivakumar, N. Srinivasamurthy, and B. L. Agrawal, "Determination of solar cell diffusion capacitance and its dependence on temperature and 1 MeV electron fluence level," *Sol. Energy Mater. Sol. Cells*, vol. 26, no. 3, pp. 169–179, 1992, doi: 10.1016/0927-0248(92)90058-W.

[22] M. Chegaar, A. Hamzaoui, A. Namoda, P. Petit, M. Aillerie, and A. Herguth, "Effect of illumination intensity on solar cells parameters," *Energy Procedia*, vol. 36, pp. 722–729, Jan. 2013, doi: 10.1016/j.egypro.2013.07.084.

[23] F. Khan, S. N. Singh, and M. Husain, "Effect of illumination intensity on cell parameters of a silicon solar cell," *Sol. Energy Mater. Sol. Cells*, vol. 94, no. 9, pp. 1473–1476, Sep. 2010, doi: 10.1016/j.solmat.2010.03.018.

[24] M. C. Jones *et al.*, "X-ray power and yield measurements at the refurbished z machine," *Rev. Sci. Instrum.*, vol. 85, no. 8, Aug. 2014, Art. no. 083501, doi: 10.1063/1.4891316.

[25] N. R. Joseph *et al.*, "Enhancements to the short pulse high intensity nanosecond X-radiator (SPHINX) pulsed power system," in *Proc. IEEE Pulsed Power Conf. (PPC)*, May 2015, pp. 1–5, doi: 10.1109/PPC.2015.7296969.